The Type Ib SN 1999dn: one year of photometric and spectroscopic monitoring⋆

S. Benetti,[1]† M. Turatto,[2] S. Valenti,[3] A. Pastorello,[3] E. Cappellaro,[1] M. T. Botticella,[3] F. Bufano,[1] F. Ghinassi,[4] A. Harutyunyan,[4] C. Inserra,[2] A. Magazzù,[4] F. Patat,[5] M. L. Pumo[2] and S. Taubenberger[6]

[1]*Osservatorio Astronomico di Padova, vicolo dell'Osservatorio 5, I-35122, Padova, Italy*
[2]*Osservatorio Astrofisico di Catania, Via S. Sofia 78, I-95123, Catania, Italy*
[3]*Astrophysics Research Centre, School of Mathematics and Physics, Queen's University Belfast, BT7 1NN*
[4]*Telescopio Nazionale Galileo, Fundación Galileo Galilei – INAF, Rambla José Ana Fernández Pérez, 7, 38712 Breña Baja, TF, Spain*
[5]*European Southern Observatory, Karl Schwarzschild-Str. 2, 85748, Garching bei München, Germany*
[6]*Max-Planck-Institut für Astrophysik, Karl Schwarzschild Str. 1, 85741 Garching bei München, Germany*

ABSTRACT

Extensive optical and near-infrared observations of the Type Ib supernova (SNIb) 1999dn are presented, covering the first year after explosion. These new data turn this object, already considered a prototypical SNIb, into one of the best observed objects of its class. The light curve of SN 1999dn is mostly similar in shape to that of other SNeIb but with a moderately faint peak ($M_V = -17.2$ mag). From the bolometric light curve and ejecta expansion velocities, we estimate that about $0.11\,M_\odot$ of ^{56}Ni were produced during the explosion and that the total ejecta mass was 4–$6\,M_\odot$ with a kinetic energy of at least 5×10^{51} erg. The spectra of SN 1999dn at various epochs are similar to those of other stripped envelope SNe showing clear presence of H at early epochs. The high explosion energy and ejected mass, along with the small flux ratio [Ca II]/[O I] measured in the nebular spectrum, together with the lack of signatures of dust formation and the moderate metallicity environment is not inconsistent with a single massive progenitor ($M_{\mathrm{ZAMS}} \geq 23$–$25\,M_\odot$) for SN 1999dn.

Key words: supernovae: general – supernovae: individual: 1999dn.

1 INTRODUCTION

In the supernova (SN) taxonomy, Type Ib SNe (SNIb) are defined as the subclass of core-collapse explosions (CC-SNe) whose early-time spectra are characterized by strong He I lines (e.g. Wheeler & Levreault 1985; Turatto, Benetti & Pastorello 2007). CC-SNe are thought to descend from massive progenitors ($M > 7$–$8\,M_\odot$) and include also the most frequent, H-dominated Type II SNe (SNII) as well as Type Ic SNe (SNIc), which appear deprived of both H and He. The physical connection among these subtypes is provided by their location almost exclusively in spiral galaxies (e.g. Hakobyan et al. 2008) and, in particular, by their association to massive star formation regions (e.g. Van Dyk et al. 1999; Anderson & Jones 2008).

An additional evidence of a link between the different subtypes of CC-SNe came with the discovery of objects, called Type IIb, that metamorphose from Type II at early stages to Type Ib later on. The prototype of this subclass is SN 1993J in M81, one of the best studied SNe at all wavelengths ever (e.g. Barbon et al. 1995; Richmond et al. 1996b).

While early-time spectra of CC-SNe can be very different as a consequence of the different configurations of the progenitors at the moment of their explosions, late-time spectra of all CC-SNe are consistently similar with strong emission lines of neutral and singly ionized O and Ca, in addition to H Balmer lines for SNII. The standard scenario is that SNIb descend from massive stars that have lost their H envelope through strong winds or mass transfer to a companion (Heger et al. 2003). If in addition to the H also the He envelope has been removed, then the SN will appear of Type Ic. For this reason, SNIb, Ic and IIb are often referred to as stripped envelope (SE) SNe.

With the improved quality of data, the differences between Types Ib and Ic have shown to be subtle, and classifications often controversial. For instance, in SN 1994I, early on considered

as the prototypical SNIc, has been found possible signature of He (Filippenko et al. 1995; Clocchiatti et al. 1996); the Type Ib SN 1999ex was characterized by weak optical He I but strong He I $\lambda\lambda 10830, 20581$ lines in the near-IR (NIR; Hamuy et al. 2002); the peculiar SN 2005bf (Folatelli et al. 2006) and SN 2008D (Mazzali et al. 2008; Modjaz et al. 2009) underwent a metamorphosis from a broad line Type Ic at early times to a typical Type Ib at later epochs. The sharp distinction between the two classes seems therefore to be replaced by a continuity of properties in He abundances and/or excitation.

The study of SE SNIb/c has received fresh impetus in the past decade because of the association of some of them, in particular the most energetic SNIc (hypernovae), with gamma-ray bursts of long duration (Galama et al. 1998; Hjorth et al. 2003; Malesani et al. 2004). More recently a few SNIc have been associated with less energetic X-ray flashes (Fynbo et al. 2004; Modjaz et al. 2006; Pian et al. 2006). An X-ray flash was also detected in the Type Ib SN 2008D, which was attributed either to shock breakout at the star surface (Soderberg et al. 2008) or to the effect of mildly relativistic jets due to the collapse of a 30 $M_\odot$ star to a black hole (Mazzali et al. 2008).

Despite this renewed interest, the objects with detailed observations remain few. In particular, it is not well ascertained if SNIb do exist as a distinct class or if there is a uniform distribution of objects from SNII to SNIc with decreasing H (and He) content in the outer layers. In this context, SN 1999dn is interesting because it has been adopted several times in the past to describe the average properties of SNIb (e.g. Branch et al. 2002; Chornock et al. 2010).

SN 1999dn was discovered by Qiu, Qiao & Hu (1999a) on two unfiltered CCD images obtained on August 19.76 and 19.82 UT, respectively, in the Wolf–Rayet (WR) galaxy NGC 7714. The SN position is RA (2000.0) = $23^h36^m14\overset{s}{.}7$; Dec. (2000.0) = $+02°09'08\overset{''}{.}8$, $9\overset{''}{.}9$ E, $9\overset{''}{.}4$ S of the galaxy nucleus (Qiu et al. 1999a), in a region of steep background variation (Fig. 1). The parent galaxy, NGC 7714, is classified as SBb peculiar, and identified by Weedman et al. (1981) as a prototypical starburst galaxy. A second SN (2007fo), has been recently discovered $2\overset{''}{.}5$ W, $12\overset{''}{.}4$ N of the galaxy nucleus (Khandrika & Li 2007), which showed similarly prominent He I lines and was also classified as SNIb (Desroches et al. 2007). An-
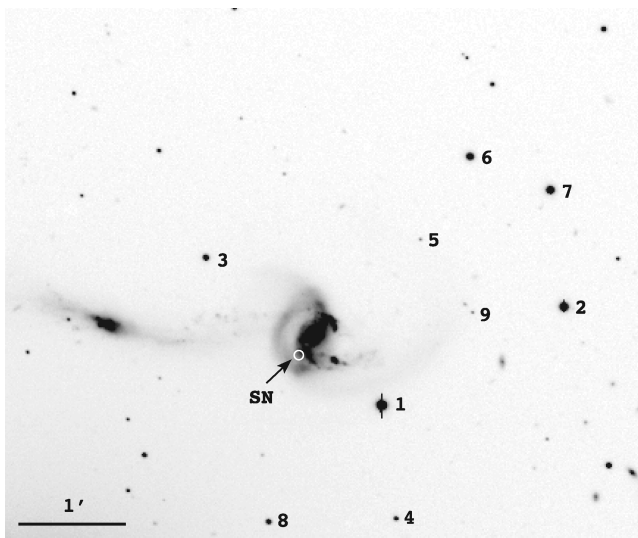
other highly reddened SN candidate was detected 2″W, 5″N of the galaxy nucleus on United Kingdom Infrared Telescope archival K-band images taken on 1998 December 5 (but not in H band, i.e. $(H - K) > 1.2$; Mattila et al. 2002).

A series of spectra of SN 1999dn has been taken soon after the discovery by different groups which classified the SN as Type Ia (Qiu et al. 1999b) and as Type Ic because of the lack or weakness of He lines (Ayani et al. 1999; Turatto et al. 1999). Few days later, the He I lines emerged and the SN was reclassified as an SNIb/c by Pastorello et al. (1999). A week later, the He I lines strengthened again making the spectra of this SN very similar to those of other Type Ib's.

Due to the early discovery, SN 1999dn was observed by several groups (Deng et al. 2000; Matheson et al. 2001). It soon became one of the best observed SNIb and a test case for extensive modelling (Deng et al. 2000; Branch et al. 2002; Ketchum, Baron & Branch 2008; James & Baron 2010). In this paper, we present original data collected at La Silla, La Palma and Asiago, and analyse them together with published material. The joint set of observations gives good multicolour photometry and dense spectral sampling, starting one week before maximum up to over two months. The SN has been recovered at late time in imaging (Van Dyk, Li & Filippenko 2003) and spectroscopy (Taubenberger et al. 2009).

2 OBSERVATIONS

UBVRIJHK′ photometry of SN 1999dn was obtained at ESO-La Silla and Telescopio Nazionale Galileo (TNG) -La Palma. 10 photometric nights were used to calibrate a local sequence of stars through comparison with photometric standard stars (Landolt 1992). In turn, the local sequence was used to calibrate observations obtained during non-photometric nights. The magnitudes of the local sequence, labelled in Fig. 1, are reported in Table 1. The estimated errors (mean standard deviation) are reported in parentheses. Due to the small field of view of Arnica only star 1 was always included in the NIR frames, which then is the reference to check the calibration of the *JHK′* photometry. The averages of the measurements of this stars in three nights are reported in the footnote of Table 1 along with their standard deviations. The moderate dispersions of the measurements and their consistency with the Two Micron All Sky Survey (2MASS) Point Source Catalogue (difference <0.2 mag) (Skrutskie et al. 2006) add confidence to the photometric calibration.

The new photometric measurements of the SN are listed in Table 2. Observations were obtained on 19 different epochs up to one year after explosion. Data reduction followed standard procedures making use of a point spread function fitting technique for

Figure 1. SN 1999dn in NGC 7714 and the sequence of local reference stars (cf. Table 1). The image is a V frame taken with TNG+Dolores on 2000 June 28. North is up and east is towards left-hand side.

Table 1. Magnitudes of the stars of the local sequence identified in Fig. 1. The photometric errors are in parentheses (in units of 10^{-2} mag).

Star	U	B	V	R	I
1[a]	15.20(05)	14.73(03)	13.84(01)	13.43(03)	12.86(02)
2	15.76(06)	15.45(04)	14.65(02)	14.20(02)	13.80(03)
3	17.91(13)	17.35(06)	16.38(02)	15.83(01)	15.36(04)
4	19.36(16)	18.58(08)	17.62(03)	17.07(09)	16.56(06)
5	22.82:	21.57(09)	19.95(07)	18.73(03)	17.44(04)
6	16.19(02)	16.20(04)	15.44(05)	14.97(03)	14.55(06)
7	15.68(05)	15.69(03)	15.03(02)	14.64(02)	14.27(02)
8	19.83(09)	18.43(08)	17.02(04)	16.13(04)	15.47(11)
9	22.71(09)	21.31(09)	19.72(04)	18.70(05)	17.58(12)

[a] $J = 12.25 \pm 0.05, H = 11.50 \pm 0.10, K' = 11.53 \pm 0.10$.

Table 2. Photometric measurements for SN 1999dn. The photometric errors are in parentheses (in units of 10^{-2} mag).

Date	JD[a]	U	B	V	R	I	J	H	K′	Instrument[b]
25/08/99	51415.71	16.93(06)	16.80(05)	16.18(04)	15.96(04)	15.82(06)				DF
28/08/99	51418.79	16.93(06)	16.81(05)	16.10(04)	15.80(04)	15.72(06)				DF
03/09/99	51424.77	17.23(06)	17.01(05)	16.24(04)	15.92(04)	15.65(06)				DF
06/09/99	51427.77	17.62(06)	17.15(05)	16.30(05)	15.95(06)	15.66(06)				DF
11/09/99	51433.49	18.59(06)	17.71(05)	16.59(04)	16.11(05)	15.69(05)				OIG
14/09/99	51435.76	18.71(06)	17.80(03)	16.64(03)	16.15(03)	15.81(04)				OIG
15/09/99	51436.50	18.97(09)	17.87(05)	16.76(03)	16.28(03)	15.85(03)				EF2
18/09/99	51439.77	19.28(09)	18.14(05)	16.91(03)	16.41(03)	15.95(03)				EF2
20/09/99	51441.58						15.38(15)	15.16(10)	14.92(30)	ARN
03/10/99	51455.48						15.78(10)	15.50(10)	15.31(20)	ARN
07/10/99	51459.47	19.99(09)	19.01(06)	17.81(05)	17.09(05)	16.63(05)				OIG
02/11/99	51485.35	20.14(15)	19.59(06)	18.32(06)	17.56(06)	16.88(06)				OIG
03/11/99	51485.58		19.53(05)	18.32(03)	17.57(05)					DF
04/11/99	51486.52		19.47(06)	18.30(03)	17.58(04)	16.95(05)				DF
10/12/99	51523.33	20.28(10)	19.89(08)	18.82(07)	18.02(07)	17.30(07)				OIG
27/12/99	51540.32		19.94(08)	19.11(07)	18.20(07)	17.59(07)				OIG
27/12/99	51540.37						17.93(20)	17.46(25)	17.64(30)	ARN
28/06/00	51723.69			22.57(35)	20.78(20)					Dol
31/08/00	51788.60			≥23.15(70)	21.93(50)					EF2

[a]240 0000+.
[b]DF = ESO/Danish 1.5-m telescope + DFOSC; OIG = Telescopio Nazionale Galileo + OIG CCD Camera; EF2 = ESO 3.6-m telescope + EFOSC2; ARN = Telescopio Nazionale Galileo + ARNICA IR Camera; Dol = Telescopio Nazionale Galileo + Dolores.

Table 3. Spectroscopic observations of SN 1999dn.

Date	Phase[a] (d)	Instrument[b]	Exp. (min)	Range (Å)	Resol. (Å)
25/08/99	−2.3	DF	45	3600–9000	9
28/08/99	+0.8	DF	45	3500–9000	9
03/09/99	+6.8	DF	45	3500–9000	9
09/09/99	+12.5	WHT	45	3200–7550	3.5
14/09/99	+17.5	EK	30	3470–7470	18
14/09/99	+17.8	EF2	15	3400–7450	14
3/11/99	+67.6	DF	120	3500–9000	10
4/11/99	+68.6	DF	120	3500–9000	10
31/08/00	+370.7	EF2	60	6000–10250	12

[a]Relative to the estimated epoch of *B* maximum (JD = 245 1418).
[b]See note to Table 2 for coding, plus WHT = WHT 4.2-m telescope + ISIS and EK = Asiago 1.8-m telescope + AFOSC.

the SN measurements. The mean photometric errors, estimated with artificial stars experiments, are given in parentheses.

The journal of the spectroscopic observations (Table 3) gives for each spectrum the date of observation (column 1), the phase relative to the adopted maximum (cf. Section 3; column 2), the instrument (column 3), the exposure time (column 4), the wavelength range (column 5) and the resolution derived from the average full width at half-maximum (FWHM) of the night-sky lines (column 6). In order to improve the signal-to-noise ratio (S/N), the average of the two spectra taken on 1999 September 3 and 4 is shown in Fig. 6, after checking that there was negligible evolution. In some spectra, the telluric absorptions have not been removed because of the lack of suitable standard stars with sufficient S/N. In other cases, it has been impossible to remove the contamination by the underlying H II region whose lines can be either under- (e.g. day +370) or over-subtracted (day +0.8). The absolute flux calibration was verified against the *B*, *V* and *R* photometry. In case of disagreement, the spectra were corrected by applying a constant factor. In fact the

slit was normally aligned along the parallactic angle, in order to minimize atmospheric differential light losses (Filippenko 1982).

3 PHOTOMETRY

The *UBVRIJHK′* light curves of SN 1999dn are shown in Fig. 2. The figure includes also the *R*-band data from fig. 27 of Matheson et al. (2001) (shifted by 15.85 mag to match our observations), the late-time observations of Van Dyk et al. (2003) and the pre-discovery limit by Qiu et al. (1999a). Only in the *R* band, the light curve has been well monitored before and around maximum. A low order polynomial fit of all points around the peak provides $JD_{max}^{R} = 2451420.5 \pm 0.5$ (1999 August 30) at $R_{max} = 15.85 \pm 0.05$ mag, in good agreement with the estimate by Matheson et al. (2001) (1999 August 31). In the other bands, the observations started a few days later and the uncertainties on the epochs of maxima are larger (cf. Table 4). Following common convention, we adopt the epoch of *B* maximum (JD 245 1418.0) as reference which is 3.5 d before the reference epoch used by Matheson et al. (2001) and later by Branch et al. (2002), Ketchum et al. (2008) and James & Baron (2010).

The peak of the light curve is asymmetric with a steep rise to maximum followed by a slow decline for about 10 d and a faster decrease afterwards. The contrast between maximum and inflection point as well as the width of the maximum light seems to be colour-dependent, with shorter wavelengths having narrower peaks and larger magnitude differences. A colour dependence is visible also in the decline rate during the late radioactive tail, longer wavelengths having steeper slopes (cf. Table 4). Only three epochs of NIR photometry are available: two during the early post-peak decline and one in the radioactive tail. Though scanty the NIR photometry has been very useful for the construction of the bolometric flux (Section 3.2).

A comparison of the colour evolutions of SN 1999dn with several other SNIb/c is illustrated in Fig. 3. All objects have been dereddened according to values reported in Table 5. An overall similarity is found among all objects of this variegated class but in the
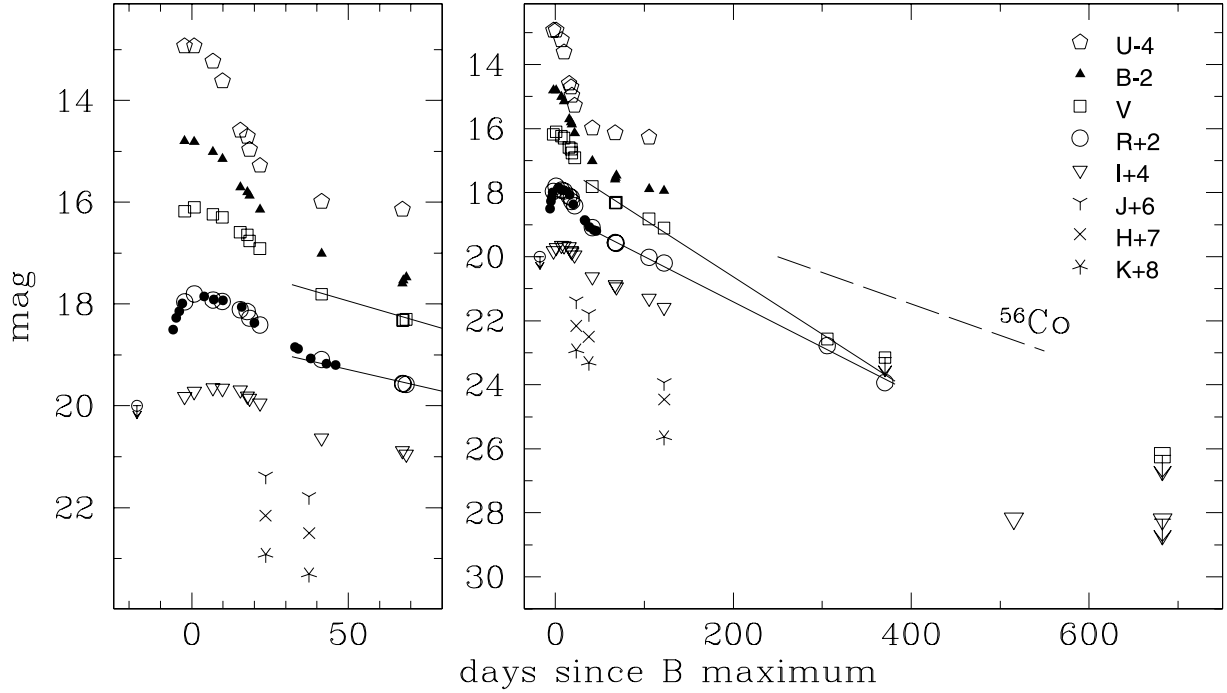
Figure 2. *UBVRIJHK'* light curves of SN 1999dn. The left-hand panel is a zoom around the epoch of maximum, while the whole evolution is shown in the right-hand panel. The *R*-band observations by Matheson et al. (2001) are reported as small filled circles, shifted to match our *R* magnitudes. The pre-discovery unfiltered limit by Qiu et al. (1999a) is reported in the *R*-band scale (open circle + arrow). Late time (>500d) *F550W* and *F814W* observations by Van Dyk et al. (2003) are reported in the *V* and *I* scale, respectively, as large symbols. To guide the eye, the late time *V* and *R* observations have been fitted by straight lines, while a dashed line is drawn to show the slope of ^{56}Co decay.

Table 4. Main data of SN 1999dn.

Position (2000.0)[a]	$23^h36^m14\overset{s}{.}81$	$+02°09^m08\overset{s}{.}4$	
Parent galaxy	NGC 7714, SBb pec[b]	With starburst[c]	
Offset w.r.t. nucleus	$9\overset{''}{.}9$ E	$9\overset{''}{.}4$ S	
Adopted distance modulus	$\mu = 32.95 \pm 0.11$		
SN heliocentric velocity	$2630 \pm 150\,\mathrm{km\,s^{-1}}$		
Adopted reddening	$E_{MW}(B-V) = 0.052^d$	$E_{tot}(B-V) = 0.10 \pm 0.05$	

	Peak time (JD−245 1000)	Peak observed magnitude	Peak absolute magnitude
U	418 ± 2	16.9 ± 0.1	-16.6 ± 0.5
B	418 ± 2	16.8 ± 0.1	-16.6 ± 0.4
V	419 ± 1	16.1 ± 0.1	-17.2 ± 0.4
R	420.5 ± 0.5^e	15.85 ± 0.05	-17.35 ± 0.40
I	424 ± 1	15.60 ± 0.05	-17.55 ± 0.35
uvoir	419.5 ± 0.5		$L_{bol} = 2.0 \times 10^{42}\,\mathrm{erg\,s^{-1}}$

Rise to max	~12 d	
Explosion day	~406	~ 1999 August 16

	Late time decline mag $(100\,\mathrm{d})^{-1}$	Interval (d)	Late time decline mag $(100\,\mathrm{d})^{-1}$	Interval (d)
U	0.37	67 –105		
B	0.81	67–122		
V	1.79	67–306	1.43	67–122
R	1.44	67–370	1.17	67–122[f]
I	1.64	67–515	1.19	67–122
uvoir	1.49	67–122		

M(^{56}Ni)	$0.11\,M_\odot$
M(ejecta)	$4–6\,M_\odot$
Explosion energy	$5.0–7.5 \times 10^{51}$ erg

[a] Qiu et al. (1999a); [b] http://leda.univ-lyon1.fr; [c] Weedman et al. (1981); [d] Schlegel et al. (1998); [e] 1999 August 30; [f] our data only.
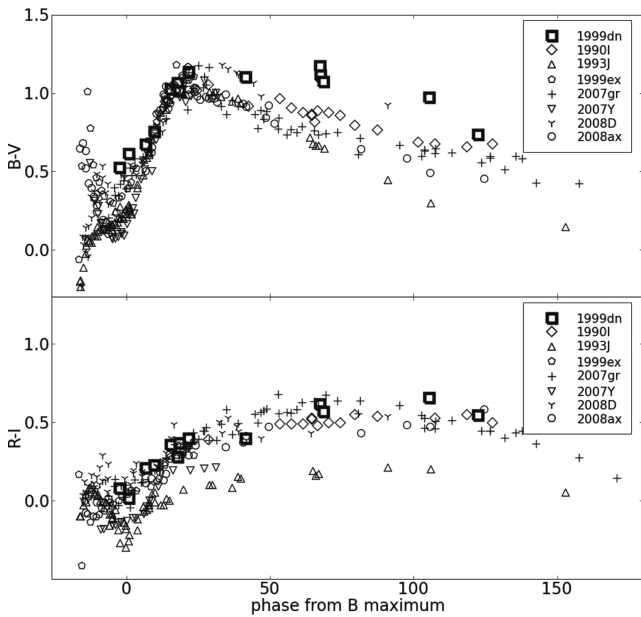
Figure 3. Top panel: comparison of the $B - V$ colour curve of SN 1999dn with those of other SE–SNe. The curves have been dereddened with the values reported in Table 5 and a standard extinction law. Bottom panel: as above, but for the observed $R - I$ colour curve ($r - i$ for SN 2007Y).

pre-maximum phase. At maximum light, the $B - V$ colours are between $+0.1$ and $+0.6$ mag and become redder afterward, reaching a maximum value (0.9–1.2 mag) at about 20 d because of the cooling due to expansion. Thereafter the $B - V$ colours slowly turn bluer due to the progressive increase of the emission line strengths. A good coverage before maximum is available only for the helium rich SNe 1993J, 1999ex, 2008D and 2008ax, which show very different behaviours. Whereas the blue band light curves of the Type IIb SN 1993J showed an early peak attributed to the emergence of the shock breakout, SN 2008ax, the other SNIIb of the sample, showed evidence of its emergence only in the very early UV light curve (Roming et al. 2009), but not in the optical (Pastorello et al. 2008; Taubenberger et al. 2010) and thus the colour curve had an opposite behaviour, starting red and turning bluer. Already one week before maximum, the $B - V$ curves of both objects reach similar values ($B - V = +0.15$ mag) and evolve similarly afterwards. The pre-maximum difference may be attributed to the fact that SN 2008ax had a more compact progenitor and a lower density wind than SN 1993J (Chevalier & Soderberg 2010). An early peak in the blue light curves is also visible in SN 2008D and possibly in SN

1999ex. Indeed both objects show early $B - V$ colours comparable to SN 1993J. However, the blue colour peak is very short in SN 1999ex and the evolution extremely fast, with the $B - V$ colour reddening by over 1 mag in only 3 d and resembling the general trend described for SN 2008ax thereafter. The behaviour of SN 1999ex leaves room for the presence of early, short shock breakout signatures also in other objects.

The colours of SN 1999dn are available only from around maximum, but the spectral evolution in the week before (cf. Section 4) indicates that the spectral energy distribution (SED) has become bluer and bluer from day −6 to maximum light, which suggests a colour evolution for SN 1999dn more similar to SNe 1999ex and 2008ax than to SN 1993J. After reaching a maximum value of $B - V$ similar to all other SNIb/c, SN 1999dn remained unusually red up to over 100 d. The adoption of an higher extinction correction might reduce the difference (cf. Section 3.1).

The $R - I$ colour evolutions of SE–SNe are smoother and remain confined between −0.3 mag at maximum and +0.7 mag later on. All objects show similar evolution and SN 1999dn is in the troop. The outlier here is SN 1993J, which remains bluer at all epochs.

3.1 Reddening and absolute magnitudes

The interstellar NaID lines arising both from our and the parent galaxy are well seen in the low-resolution spectra at about 5893 and 5945 Å, respectively. Therefore the reddening of SN 1999dn cannot be neglected. Schlegel et al. (1998) give a galactic reddening $E_{MW}(B - V) = 0.052$ mag in the direction to NGC 7714. We have measured the equivalent widths (EWs) of the NaID components in the spectra of SN 1999dn on the spectrum of highest S/N and resolution (WHT on September 9, res. 3.5 Å) and found an $EW_{MW}(NaID) \sim 0.51$ Å and $EW_{N7714}(NaID) \sim 0.45$ Å. These values are in good agreement with the average of EW measurements performed on all other available spectra with no evidence of significant time evolution. Assuming that the gas/dust properties in NGC 7714 and the Galaxy are the same, we estimate a total reddening $E_{tot}(B - V) = 0.098$ mag. A similar value $E_{tot}(B - V) = 0.131$ mag is obtained by using the average relation between $E(B - V)$ and EW(NaID) (Turatto, Benetti & Cappellaro 2003). Finally, the match of the colour curves of SN 1999dn to those other SE SNe (cf. Section 3) suggests a consistent, though formally slightly higher reddening, $E(B - V) \sim 0.15$. Throughout this paper, we adopt for SN 1999dn a total reddening $E_{tot}(B - V) = 0.10 \pm 0.05$ mag ($A_V = 0.31$ mag).

Since there is no direct measurements of the distance to NGC 7714, we use the Hubble's law. From the wavelength of the

Table 5. SE SNe used for colour and bolometric luminosity comparison.

| SN	Host galaxy	SN type	$E_{tot}(B - V)$	$(m - M)$	Main references
1999dn	NGC 7714	Ib	0.10	32.95	Section 3.1 of this paper
1990I	NGC 4650A	Ib	0.16	32.90	Elmhamdi et al. (2004)
1993J	NGC 3031	IIb	0.30	27.80	Barbon et al. (1995); Richmond et al. (1996b)
1994I	NGC 5194	Ic	0.45	29.75	Richmond et al. (1996a); Dessart et al. (2008)
1999ex	IC 5179	Ib	0.28	33.19	Stritzinger et al. (2002)
2004aw	NGC 3997	Ic	0.37	34.17	Taubenberger et al. (2006)
2005bf	MCG +00−27−5	Ib/c	0.05	34.46	Folatelli et al. (2006)
2007Y	NGC 1187	Ib	0.11	31.13	LEDA, Stritzinger et al. (2009)
2007gr	NGC 1058	Ic	0.09	29.84	Valenti et al. (2008a); Hunter et al. (2009)
2008D	NGC 2770	Ib	0.66	32.29	Mazzali et al. (2008); Modjaz et al. (2009)
2008ax	NGC 4490	IIb	0.40	29.92	Pastorello et al. (2008); Taubenberger et al. (2010)
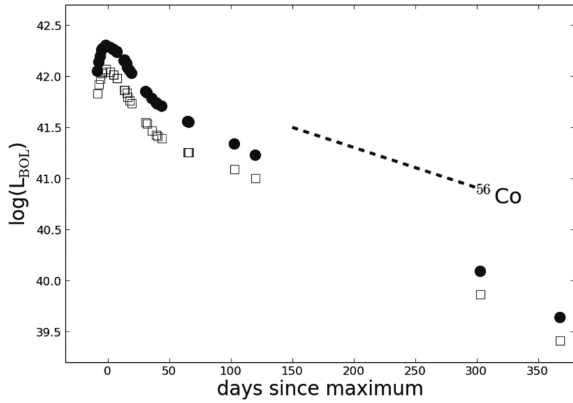
Figure 4. *UBVRIJHK'* bolometric (filled circles) and *UBVRI* (open squares) light curves of SN 1999dn. The points on the rising branch and those after four months past maximum are largely based on extrapolations (assuming constant colours) and should be regarded as uncertain. The slope of ^{56}Co to ^{56}Fe decay is also displayed for comparison.

interstellar NaID absorption features we derive a recession velocity of $2630 \pm 150\,\mathrm{km\,s^{-1}}$, which is consistent with the heliocentric radial velocity reported by LEDA[1] ($2797 \pm 16\,\mathrm{km\,s^{-1}}$). LEDA provides also a velocity corrected for the Local Group infall into the Virgo cluster $v_{\mathrm{Vir}} = 2798\,\mathrm{km\,s^{-1}}$. Adopting $H_0 = 72\,\mathrm{km\,s^{-1}\,Mpc^{-1}}$, we derive a distance modulus $\mu = 32.95$ mag which is used throughout this paper.[2]

Adopting the above mentioned values for extinction and distance, we obtain the following absolute magnitudes at maximum $M_U = -16.6 \pm 0.5$, $M_B = -16.6 \pm 0.4$, $M_V = -17.2 \pm 0.4$, $M_R = -17.35 \pm 0.40$ and $M_I = -17.55 \pm 0.35$, where in the computation of the errors we adopted an uncertainty of $\pm 250\,\mathrm{km\,s^{-1}}$ on the Hubble distance modulus due to possible peculiar motion.

We note that, after rescaling to a common distance scale, our determination of M_V is 0.5 mag brighter than that derived by Richardson, Branch & Baron (2006), but in good agreement with the mean value of $M_R = -17.01 \pm 0.41$ given by Li et al. (2010) for a sample of six SNIb, SN 1999dn included. In comparison to the subsamples studied in Li et al., SN 1999dn remains about 0.80 mag brighter than their unweighted mean for the *normal* SE SNe (SNIc+Ib+IIb).

3.2 Bolometric light curve

With the available photometry, it has been possible to build the *UBVRIJHK'* bolometric light curve up to 1 yr (Fig. 4). When magnitudes in a bandpass were not available in a given night, the values were linearly interpolated. The light curves with a short temporal extension, e.g. those in the NIR, were extrapolated assuming constant colours. For this reason, the bolometric flux during the rising branch and those at the latest epochs are based mainly on *R*-band observations and should be regarded as uncertain. The photometry was corrected for extinction using $R_V = 3.1$. At the effective wavelengths of each filter monochromatic fluxes were computed; these were then integrated from the *U* to *K'* bands using the trapezoid approximation, and converted to luminosity. The peak of the bolo-

---

[1] http://leda.univ-lyon1.fr
[2] A similar value ($\mu = 32.84$) is obtained adopting the distance relative to the Virgo cluster in the 220 model (Kraan-Korteweg 1995) with $D(\mathrm{Virgo}) = 15.3\,\mathrm{Mpc}$ (Freedman et al. 2001).

metric light curve is reached between the *V* and the *R* maxima on $\mathrm{JD}^{\mathrm{bol}}_{\mathrm{max}} = 245\,1419.5 \pm 0.5$ at a luminosity $L_{\mathrm{bol}} = 2.0 \times 10^{42}\,\mathrm{erg\,s^{-1}}$.

The contribution of the NIR bands is substantial at all the epochs in which NIR data are available ($L_{JHK}/L_{uvoir} = 0.5$, 0.5 and 0.4 at days 20, 40 and 121, respectively). This is more than a factor of 2 larger than the value derived for SNIb 2007Y (Stritzinger et al. 2009) and for SN 2008D (Modjaz et al. 2009), but similar to values derived for SNIIb 2008ax (Taubenberger et al. 2010). In the photospheric phase, the optical+NIR SED deduced from SN 1999dn photometry is consistent with a blackbody energy distribution with temperatures as derived from optical spectra (cf. Section 4). The decline rate between 67 and 122 d is 1.49 $\mathrm{mag}\,(100\,\mathrm{d})^{-1}$, close to the average value of Type Ia SNe. This value is significantly larger than the decline rate of 0.98 $\mathrm{mag}\,(100\,\mathrm{d})^{-1}$ predicted if all the energy from the decay of ^{56}Co into ^{56}Fe was fully thermalized. No significant slope variation is observed up to day 370 ($\gamma_{uvoir} = 1.65$ [67–305 d]).

In Fig. 5, we compare the bolometric light curve of SN 1999dn with those of other SE SNe. Unfortunately, not all have coverage from optical to NIR wavelengths. The comparison has been done both for the extended *uvoir* (*UBVRIJHK'*, top panel) and the optical-only (*UBVRI*, bottom panel) bolometric curves.

The rise to maximum can be very different. The Type IIb SN 1993J shows an early bright spike about 20 d before a broader secondary maximum. For the other SNIb caught early-on, SN 1999ex (bottom panel), the bolometric light curve shows just an hint of the shock breakout.

For the peculiar SN 2005bf, a slow rise to a first maximum is observed followed about 25 d later by a second brighter maximum. The Type Ib SN 2007Y and the Type Ic SNe 1994I, 2004aw and 2007gr were not detected sufficiently early after the explosion and do not show any feature in the rising branch. The first reliable photometry of SN 1999dn has been obtained 6 d before *B* maximum
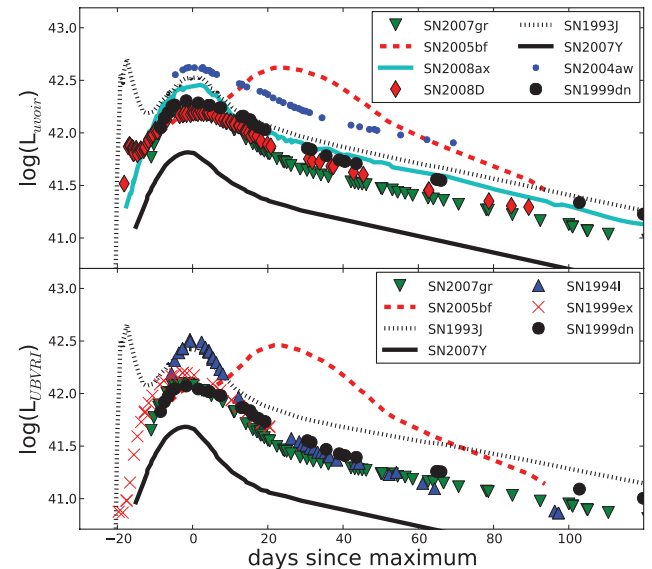

Figure 5. Comparison of the bolometric light curve of SN 1999dn with those of other Type Ib/c SNe. The phase is from *B* maximum. The comparison based on the whole optical–NIR (*uvoir*) domain is in the top panel, that based on the *UBVRI* bands (*uBgVri* for SN 2005bf, *UuBgVri* for SN 2007Y) in the bottom panel. The SN distances and reddening are reported in Table 5. Note that with the adopted distance and reddening SN 1994I is among the brightest objects. Small misalignments in the epochs of maxima are due to different choices of the reference epochs.
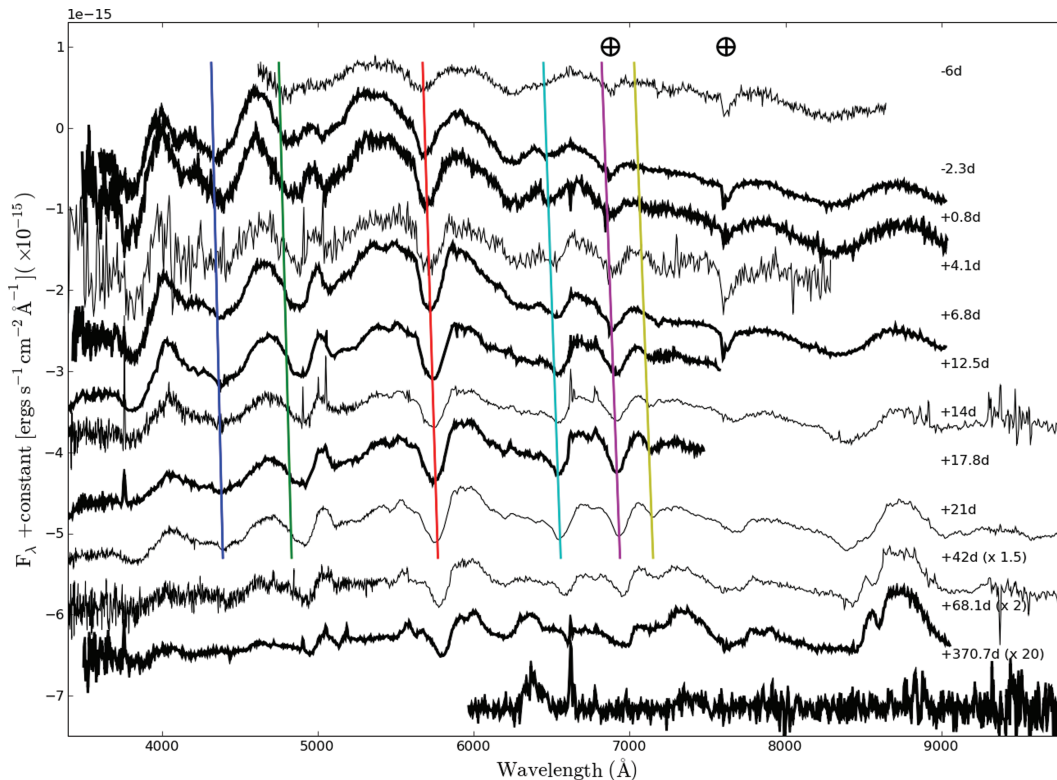
Figure 6. The overall spectral evolution of SN 1999dn [including spectra by Deng et al. (2000) and Matheson et al. (2001) as thin lines]. The wavelength is in the observer rest frame and the flux is not corrected for reddening. The ordinate refers to the top spectrum; other spectra are shifted downwards with respect to the previous by 1.2×10^{-15} (second spectrum) and 0.6×10^{-15} erg s^{-1} cm^{-2} Å^{-1} (others). The spectra taken on November 3 and 4 have been averaged, while for September 14 only the EFOSC2 spectrum is displayed. Vertical lines correspond to the positions of He I $\lambda\lambda\lambda\lambda\lambda\lambda$4472, 4921, 5876, 6678, 7065 and 7281, with expansion velocities of 13 000 km s^{-1} at the earliest epoch and then slowing down with time. Each spectrum is labelled with the phase with respect to the B maximum (JD = 245 1418.0). For clarity, the last three spectra have been multiplied by the factors reported in parentheses. Telluric features are marked with the Earth symbol.

(8.5 d before R maximum), while the available pre-discovery limit does not put stringent constraints on the date of explosion. The direct comparison with other SNIb/c suggests a rise time (relative to B maximum) similar to SN 2007gr, i.e. 11.5 ± 2.0 d (Hunter et al. 2009).

The contribution of the *JHK'* bands to the bolometric flux of SN 1999dn stands out: while in the *UBVRI* domain it has almost the same luminosity as the Type Ic SN 2007gr, in the *uvoir* it outpasses it by about 0.12 dex.

The asymmetric peak of SN 1999dn, with a relatively fast rise and slow decline, reminds of the behaviour of SN 2007gr, but with even slower decline. After maximum, the bolometric light curve remains relatively broad and closely resembles in shape with that of SN 2004aw, but remains about 0.3 dex fainter at all epochs . This simple comparison indicates that adopting the Arnett model (Arnett 1982) at the early times, when the diffusion approximation is valid, the amount of ^{56}Ni synthesized in the explosion of SN 1999dn is between 0.10 and 0.15 M$_\odot$ [$M_{\rm Ni}$(2007gr) = 0.076 M$_\odot$, Hunter et al. (2009); $M_{\rm Ni}$(2004aw) = 0.30 M$_\odot$, Taubenberger et al. (2006)]. Broad light curves are indicative of large diffusion time and hence of either a large ejected mass or a small kinetic energy. The comparison of the expansion velocity of SN 1999dn (cf. Section 4.1) with other SE SNe suggests that the long diffusion time is due to a large ejecta mass of SN 1999dn much larger than that of the narrow-peak SN 1994I (cf. Fig. 5). A more detailed discussion of the explosion parameters is given in Section 5.

4 SPECTROSCOPY

The entire spectroscopic evolution of SN 1999dn from about one week before maximum to over 1 yr is illustrated in Fig. 6, thanks to the spectra listed in Table 3 and those published by Deng et al. (2000) and Matheson et al. (2001). The SN evolution is therefore well sampled at all crucial phases. We stress again that the phases adopted here are relative to the date of B maximum (JD 245 1418.0) and differ from those used in previous papers (cf. Section 3).

The first spectrum (-6 d, August 21) has been subject to deep scrutiny. Deng et al. (2000) have modelled it with SYNOW using a blackbody temperature $T_{\rm bb} = 7500$ K and photospheric velocity $v_{\rm ph} = 16\,000$ km s^{-1}. Besides the broad absorptions at 4750 and 4950 Å (rest frame) due to Fe II, and at about 8200 Å due to Ca II IR, the spectrum is dominated by the He I $\lambda\lambda$5876 and 7065 which contribute to the strong 5620 and 6820 Å features. The broad absorption at about 6200 Å has attracted the attention of Deng et al. and other modellers and will be extensively discussed in Section 4.1. This spectrum has been modelled also by Branch et al. (2002) who used SYNOW with line optical depths varying as v^{-n} and $n = 8$ instead of e^{-v/v_e} ($v_e = 1000$ km s^{-1}) as in Deng et al. (2000). The spectrum was well reproduced with $T_{\rm bb} = 6500$ K and $v_{\rm ph} = 14\,000$ km s^{-1} and the same contributing ions. Ketchum et al. (2008) modelled this and the other spectra around maximum with their non-local thermodynamic equilibrium (non-LTE) code PHOENIX trying both a standard solar and a three times higher metallicity. Although they

adopted a smaller extinction [$E(B - V) = 0.052$ mag] and later explosion epoch (12 d before August 31) with respect to the values that we now consider more realistic (cf. Table 4), their fit is good also for the non-thermal He I lines. The other features were identified with Ca II, Fe II and O I. Similar results were obtained also by James & Baron (2010) who correct the spectrum only for galactic extinction (Baron, private communication). Their model parameters ($T_{mod} = 6000$ K and $v_0 = 11\,000$ km s^{-1}) are slightly smaller than the values ($T_{bb} = 6700 \pm 200$ K and $v_{ph} = 12\,800$ km s^{-1}) we derive by fitting the dereddened spectrum. Note that our T_{bb} is a colour temperature, different from T_{mod} which is much closer to an effective temperature, while the aforementioned SYNOW T_{bb} has little physical significance (Deng 2000).

Our new observations provide a good coverage of the epoch of maximum with spectra on days –2.3 and +0.8. At this phase the object has become bluer and hotter, reaching $T_{bb} = 9100$ and 7800 K, respectively. The line contrast is now higher with more pronounced absorption troughs and broad emissions. The He I lines have become stronger so that the $\lambda6678$ line is clearly identified in addition to the $\lambda\lambda5876$ and 7065 lines. In the blue strong Ca II H&K and Fe II lines are visible which indicate photospheric expansion velocities $v_{ph} = 10\,400$ and $10\,000$ km s^{-1}, respectively.

The next available spectrum on day +4.1, August 31, though quite noisy, has been modelled using both SYNOW ($T_{bb} = 7000$ K and $v_{ph} = 12\,000$ km s^{-1}, Deng et al. 2000; $v_{ph} = 10\,000$ km s^{-1}, Branch et al. 2002) and PHOENIX (Ketchum et al. 2008) giving an effective temperature of 6000–6500 K and $v_{ph} = 10\,000$ km s^{-1}. The features are well fit by the same ions as on day -6 (Ca II, Fe II, He I and O I). The model with standard solar metallicity reproduces fairly well also the He lines both in absorption and in emission. Again the best-fitting temperature by James & Baron (2010) is lower ($T_{mod} = 5250$ K). Our blackbody fit to the dereddened spectrum of day +4.1 provides $T_{bb} \sim 6400$ K which is lower than the values derived for the two bracketing epochs ($T_{bb} = 7800$ and 7000 K for days +0.8 and +6.8, respectively) possibly because of a poor instrument response calibration. The position of the Fe lines at about 5000 Å corresponds to $v_{ph} = 10\,000$ km s^{-1}, in good agreement with the velocities derived in the spectral modelling.

Of much better quality (S/N > 100) is the spectrum obtained on day +6.8. The fit to the SED provides $T_{bb} = 7000$ K, and the expansion velocity from the Fe II lines decreases to $v_{ph} = 8600$ km s^{-1}.

In the following week the evolution slows down. Two spectra are available on day +12.5 and +14, the former with an excellent S/N (=150) and resolution (3.5 Å), the latter with wider spectral range (Matheson et al. 2001). Our analysis provides a similar temperature, $T_{bb} \sim 5500$ K in both spectra, but significantly different photospheric velocities ($v_{ph} = 6400$ and 4900 km s^{-1}, respectively). Both the Galactic NaID lines as well as those originating in the host galaxy are well resolved, as mentioned in Section 3.1. He I $\lambda5876$ is very broad and possibly heavily contaminated by NaID. Also the lines at $\lambda\lambda6678$ and 7065 clearly stand out, whereas others ($\lambda\lambda4472$ and 7281) are less pronounced (the former probably blended with Mg II). The well-developed He I lines make the spectrum closely resemble that of prototypical SNIb. Ketchum et al. (2008) have studied the spectrum of day +14: again the solar metallicity model fits the observations better, though the Ca II and He I absorptions are too strong. Ti II starts to contribute significantly to the Fe II dominated region below 5000 Å.

Three spectra have been obtained on September 14 (from days +17.5 to +17.8) at different telescopes (cf. Table 3 and Deng et al. 2000). The SEDs of our two spectra are similar ($T_{bb} = 4800$ K) but the S/N of that obtained with EFOSC2 (plotted in Fig. 6) is

definitely higher. The Deng et al. (2000) spectrum, significantly bluer ($T_{bb} = 5700$ K), has been used in the modelling both by Deng et al. (2000) and Ketchum et al. (2008). Again the standard composition model seems to be preferred though with too strong He I and Ca II absorptions. The index n of the density profile $\rho \propto r^{-n}$ was decreased from 13 to 10 to improve the fit.

The subsequent spectra (days +21 and +42, i.e. September 17 and October 8) come from Matheson et al. (2001). At both epochs, the main features and the SEDs have not changed significantly with respect to day +18. We measure $T_{bb} \sim 4900$ K on the dereddened spectrum, in good agreement with the temperature adopted in the modelling (respectively 4800 and 4600 K; Branch et al. 2002; James & Baron 2010). The measured expansion velocities are $v_{ph} = 5500$ and 4600 km s^{-1}, respectively. In the latter spectrum, one can notice that the CaIR triplet starts to be resolved with an absorption at about 8360 Å, corresponding to a velocity v(Ca II) ~ 7700 km s^{-1}. As the temperature of the SN has decreased to about 5500 K, the region bluer than 5000 Å is largely dominated by Ti II lines (Ketchum et al. 2008). This explains why the high-metallicity model fails to reproduce the observations causing too strong absorptions.

The latest spectrum of the photospheric series (day +68) is the average of two spectra taken with the same instrument on two consecutive nights. The He I lines are still visible as well as the underlying continuum ($T_{bb} = 4400$ K). Nevertheless, the progressive transition to the nebular phase can be recognized. In particular, the broad [O I] $\lambda\lambda$ 6300, 6364 and [Ca II] $\lambda\lambda$ 7291, 7323 ([O II] $\lambda\lambda$ 7320, 7330) features start to appear clearly .

The characterizing features of the nebular spectra of SNIb/c are, indeed, [O I] and [Ca II] emission lines. These are well developed at the epoch of our last spectroscopic observation (day 371). Once deblended into its two components, the [O I] line has an overall Gaussian profile centred slightly redward of the rest-frame position (6309 Å) with FWHM ~ 4500 km s^{-1}, though the relatively poor S/N still allows for the presence of additional structures in the line profile (Taubenberger et al. 2009). In any case, there is no evidence for profile distortion or a blueshift due to dust formation as detected in other objects (e.g. SN 1990I; Elmhamdi et al. 2004) in the same [O I] line.

4.1 The expansion velocities and the presence of hydrogen

Hydrogen lines at early epochs distinguish the spectra of SNIIb from other SE SNe. Actually, faint H lines have been revealed unambiguously in the Type Ib SN 2000H and, with lower confidence, in other SNIb (Branch et al. 2002; James & Baron 2010). These authors concluded that H is present with low optical depths in SNIb in general and that it is located in a detached shell with velocities as high as 11\,000–13\,000 km s^{-1}. In this context, some attention has been paid in the previous spectral analyses of SN 1999dn (Deng et al. 2000; Branch et al. 2002; Ketchum et al. 2008; James & Baron 2010) to a broad feature present in the spectra around maximum at about 6200 Å.

The feature seen in the first epoch (day -6) was attributed by Deng et al. (2000) to Hα or C II $\lambda6580$, arising in a detached layer with velocity $v = 19\,000$ or $20\,000$ km s^{-1}, respectively. Also Branch et al. (2002) interpreted the feature as due to Hα from a detached layer of H at 18\,000 km s^{-1}. The possible alternative identification as Si II, proposed by Woosley & Eastman (1997) for SN 1984L, results in an expansion velocity (7300 km s^{-1}) significantly lower than that of any other ion and is, therefore, considered unlikely. Similar identifications were proposed for the spectra of day +4.1 (Hα, Branch et al. 2002; possibly blended with C II, Deng

et al. 2000) and days +17 and +21 (C II, Deng et al. 2000, or Fe II, Branch et al. 2002). The spectra were revisited by Ketchum et al. (2008). They found that at early times, when the 6200-Å feature is strong and broad, an uniform atmosphere of three times solar metallicity, devoid of any H, could provide a plausible explanation, making the feature a blend of Fe II lines and Si II λ6355. At later times, the feature splits into multiple, distinct, weaker features, and solar metallicity fits better. However, they admit that higher metallicity in the outer envelope (as seen in the early-time spectra) is difficult to explain, also in the light of our direct determination of a somewhat subsolar metallicity for the SN environment (cf. Section 5). The simpler interpretation of the 6200-Å feature, therefore, seems to be the presence of H. The new, specific analysis by James & Baron (2010) confirms this identification and suggests an H mass of $M_H \leq 10^{-3}$ M$_\odot$ in an outer shell of solar composition above the He core.

With this work we add new, high S/N spectra around maximum, and readdress the issue of the possible presence of H. In Fig. 7, we have zoomed into the Hα (right-hand panel) and Hβ (left-hand panel) regions of the best available spectra. To guide the eye in the right-hand panel, we have drawn two vertical dashed lines corresponding to velocities of −16 900 and −12 100 km s^{-1} at the earliest epoch, assuming the Hα identification. The dotted line at lower velocity indicates the position of He I λ6678 (the same as in Fig. 6). The line is tilted to roughly match the velocity decrement. Contrary to He I, the 6200-Å feature appears at constant velocity (−16 900 km s^{-1}) up to maximum light, while a notch at about −12 000 km s^{-1} might be present. Should these features be due to single lines and not to the conspiring effect of line blending (e.g. Fe II and Si II), the constancy in expansion velocity is an indication of detached layers. Note that the blue wing of the strong He I λ5876 line extends outward to about −18 000 km s^{-1} on day −6

and −15 500 km s^{-1} on day +0.8, close to the estimated velocity of the fastest H layer.

By day +6.8, the broad 6200-Å feature has disappeared. Starting on day +12.5 down to day +21, two distinct, resolved features spaced by about the same amount as before are clearly visible. They were noted by Ketchum et al. (2008) who suggested the same possible interpretation with Fe II, Si II, C II and Ti II. The slower component, if identified with Hα, shows marginally higher velocity than He I λ6678 and slows down with time at the same rate (~1000 km s^{-1} in 10 d).

To check whether this pair of lines are due to H, we have drawn two lines at corresponding velocities on the left-hand panel of Fig. 7, relative to Hβ. Although the Hβ optical depth is expected to be significantly smaller than that of Hα, we note that possible signatures of Hβ are recognizable at the expected positions in the spectra of days −2.3 and +12.5, the latter having the best S/N and spectral resolution. Though not compelling, we consider this an additional evidence that H is present in the spectrum of SN 1999dn both in a detached layer above the photosphere and mixed with He I.

A 6250-Å feature was identified as Hα in the early spectra of the peculiar SN 2005bf at comparable velocity (~−15 000 km s^{-1}) on the basis of the detection of similar tiny features at the corresponding position of Hβ (Folatelli et al. 2006). Also Ca II and Fe II lines had components with similar expansion velocity. For this reason, we have investigated the possible presence of high velocity features for both these ions also in SN 1999dn. In Fig. 8, the spectral regions of interest are plotted in analogy to those in Fig. 7. Broad and shallow Fe II lines seem present early on also in SN 1999dn at about −14 000 km s^{-1}, a velocity exceeding that measured for He I (−12 700 km s^{-1}) and expected for the photosphere on day −6. The Fe II lines are easily detected at smaller velocity in the following spectra. Strong, broad Ca II IR triplet absorption is detected at a velocity comparable to that of He I. In the spectra of highest S/N (days +6.8 and +14), one may also see another component about
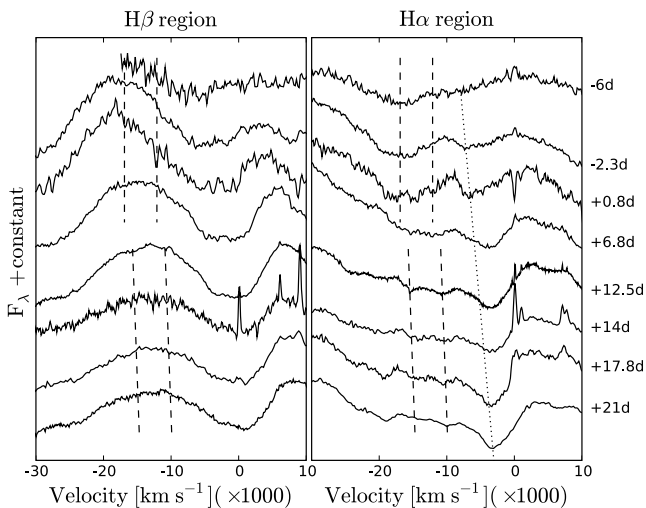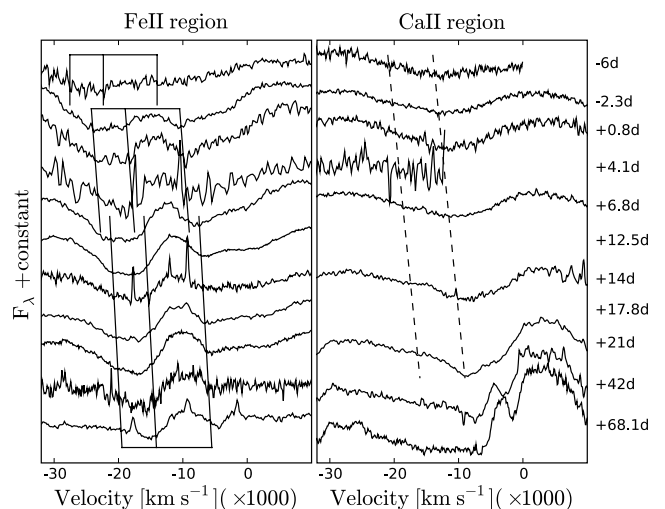

Figure 7. Zoom of the 4600 Å (left-hand panel) and 6200 Å (right-hand panel) spectral regions during the first weeks of evolution of SN 1999dn. The *x*-axes are in expansion velocity coordinates with respect to the rest-frame positions of Hβ and Hα, respectively. The phases relative to *B* maximum light are indicated on the right axis. To guide the eye, two dashed vertical lines are drawn in the spectra around maximum, corresponding to expansion velocities of about 16 900 and 12 100 km s^{-1}. After day +12.5, the broad 6200 Å feature is replaced by two narrower and weaker features which slightly slow down with time. Corresponding lines are drawn also in the left-hand panel relative to Hβ. The dotted line in the right-hand panel is drawn at the position of He I λ6678.

Figure 8. Zoom of the Fe II (left-hand panel) and Ca II IR (right-hand panel) spectral regions during the first months of evolution of SN 1999dn. In the left-hand panel, the approximate positions of Fe II λλλ4924, 5018 and 5169 are marked. The velocity reported on the abscissa refers to the λ5169 line and ranges from −14 000 to −5500 km s^{-1} from day −6 to day 68 past *B* maximum. In the right-hand panel, two dashed lines are drawn to guide the eye for the main component (right) and the possible high-velocity feature (left) of Ca II.
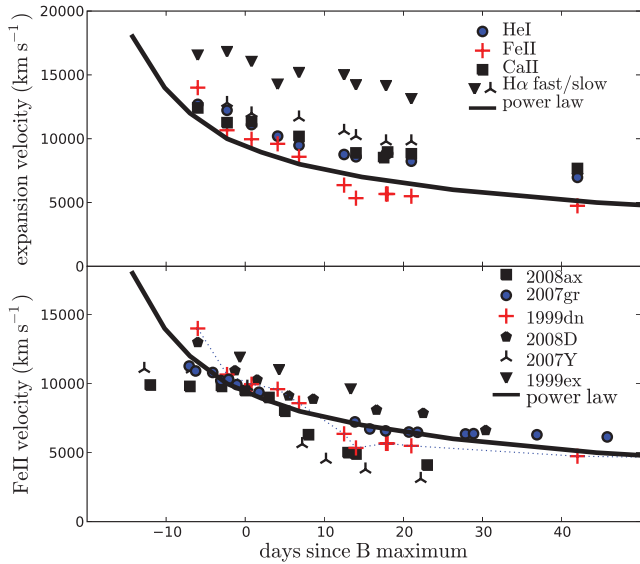
4.2 SN 1999dn and other SE SNe

We have compared the spectra of SN 1999dn with those of other SNe by means of GELATO, the spectra comparison tool developed by Harutyunyan et al. (2008) which compares input spectra with those present in our archive. Not unexpectedly, the best match is always with those of other SE SNe. In Fig. 10, we show the comparison with a number of well-studied objects during the pre-maximum and maximum phase. At these epochs, the objects that match SN 1999dn best are the extensively studied SNIIb SN 2008ax (Pastorello et al. 2008; Chornock et al. 2010; Taubenberger et al. 2010) and the energetic SN 2008D (Mazzali et al. 2008; Modjaz et al. 2009).

For the first spectrum of SN 1999dn (-6 d), the closest match is with SN 2008ax on days -9 and -8 (Pastorello et al. 2008; Taubenberger et al. 2010). The strong Hα, which unequivocally marks the presence of H in SN 2008ax at this epoch, corresponds in position to the 6200-Å feature of SN 1999dn. Note, however, that the spectra of SN 2008ax that best match those of SN 1999dn are at an earlier phase, probably because of a faster expansion velocity of SN 1999dn. At this epoch, the numerical match with SN 2008D is poorer because its expansion velocity at such epoch is even higher (Mazzali et al. 2008). There is also a general resemblance to SN 2007Y, but the expansion velocity of SN 1999dn is significantly larger.

Also at maximum, SN 1999dn best matches SN 2008D and SN 2008ax before their B maxima. The SED of SN 1999dn, however, is slightly redder. The 6200-Å feature corresponds to the fast blue wing of the Hα absorption of SN 2008ax.

Figure 9. Top panel: velocity evolution of the He I, Fe II, Ca II IR and Hα lines of SN 1999dn in the photospheric phase. The crosses are the averages of the velocities derived from the minima of Fe II lines, adopted as indicators of the photospheric velocity; the circles the average velocities of He I lines; the triangles (starred triangles) the velocity of the *fast* (*slow*) component of Hα, and the squares the velocity of the Ca II IR triplet. Bottom panel: comparison of the velocity evolution of the Fe II lines in several SE SNe. In both panels, the curve is the power-law fit from Branch et al. (2002).

5000 km s^{-1} faster but the first detection of high-velocity features of Ca II starting at this epoch makes the identification unlikely. We conclude that, in addition to Hα, there is evidence of weak high-velocity Fe II features before maximum.

In Fig. 9 (top panel), we summarize the evolution of the line velocities as a function of time. The standard deviation of the velocities derived for He I lines is $\sigma = 400$–700 km s^{-1}, possibly due to blending of various lines (e.g. NaID for $\lambda5876$, contamination by telluric features for $\lambda7065$, or by narrow Hα emission of the parent galaxy for $\lambda6678$). We estimate uncertainties of the same order for the possible H lines because of their weakness. The photospheric velocity of SN 1999dn is in agreement with those of other normal SNIb (Branch et al. 2002) and is well fitted by the power law, $v_{ph} \propto t^{-2/(n-1)}$ with $n = 3.6$. As for other SNIb, He I seems to be undetached at the first epoch but detached afterward. The lowest velocity of the He I layer is measured at about 6000 km s^{-1}. The faster H is detached at all epochs with velocity ranging between 17 000 and 13 000 km s^{-1}. The slower H component remains about 1500 km s^{-1} faster than He I at all epochs. The two H components somehow bracket the H velocities of other SNIb reported in fig. 23 of Branch et al. (2002).

The bottom panel of Fig. 9 compares the Fe II velocity of SN 1999dn with those of other SE SNe. SN 1999dn has an expansion velocity smaller than SN 1999ex but higher than other objects, e.g. SN 2007Y. Only at early phases, the velocity seems to deviate from the power-law fit by Branch et al. (2002). At these early phases, the expansion velocity is, in fact, more similar to that shown by the energetic SN 2008D. The overall normal velocity behaviour indicates that the broad (slowly evolving) light curve of SN 1999dn after the peak is probably not due to a low expansion velocity but to a larger ejected mass.
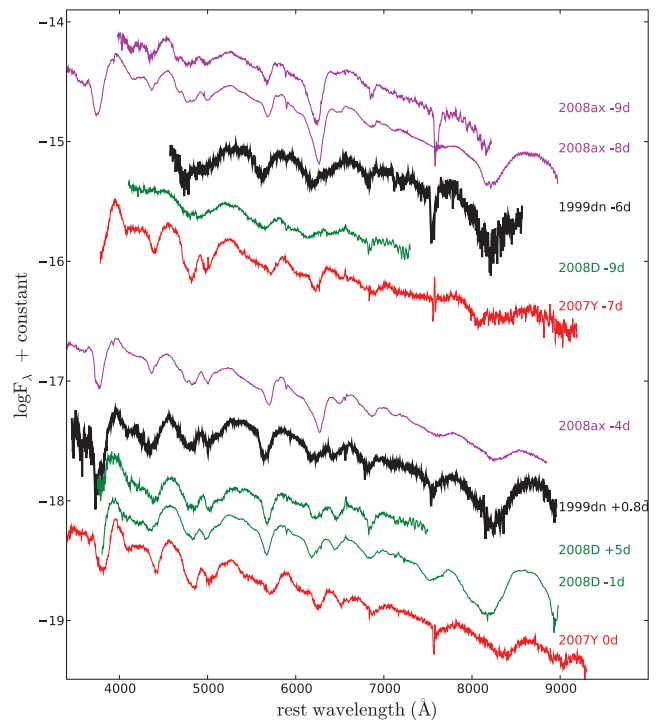

Figure 10. Comparison of the pre-maximum (-1 week, top) and maximum-light (bottom) spectra of SN 1999dn with those of other SE SNe. The spectra are plotted in the SN rest frame and dereddened according to Table 5. The phase relative to the B maximum of each object is reported close to the SN identifier. The spectra come from Mazzali et al. (2008) and Valenti et al. (in preparation) for SN 2008D, from Pastorello et al. (2008) and Taubenberger et al. (2010) for SN 2008ax, from Stritzinger et al. (2009) for SN 2007Y, and from Deng et al. (2000) and this paper for SN 1999dn.
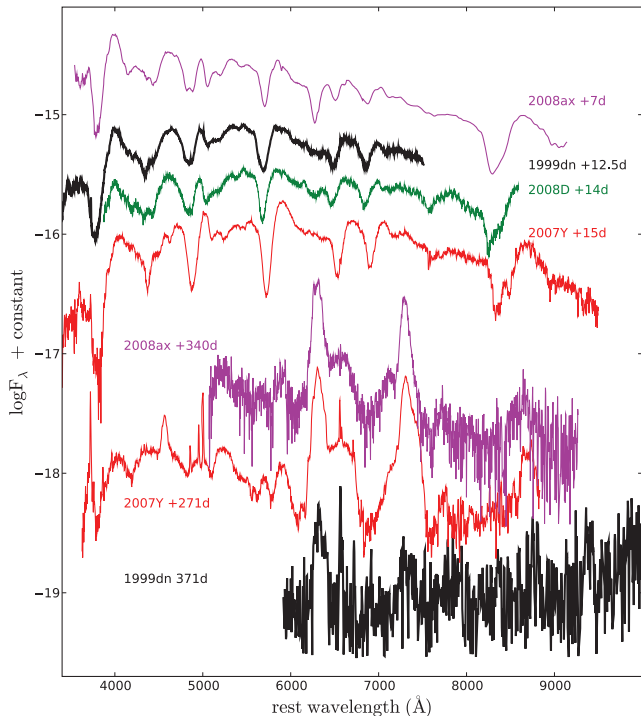
Figure 11. As in Fig. 10 but about 2 weeks (top) and 1 yr (bottom) post-maximum. The spectra come from Modjaz et al. (2009) for SN 2008D, Taubenberger et al. (2010) for SN 2008ax, Stritzinger et al. (2009) for SN 2007Y and this paper for SN 1999dn.

The comparison after maximum is shown in Fig. 11. On day +12.5 (top), the spectra of all objects are very similar. While Hα in SN 2008ax is still very strong, the 6200 features of both SN 1999dn and SN 2007Y have dimmed and two notches are left where the broad absorption was before (cf. Fig. 7). Again, due to smaller expansion velocity (cf. Fig. 9), the absorptions in SN 2007Y are redder than in SN 1999dn.

A late-time (371 d) red-grism spectrum has been obtained for SN 1999dn (Fig. 11 bottom). In both SN 2008ax and SN 2007Y, a broad shoulder on the red edge of [O I] $\lambda\lambda$6300, 6364 is clearly visible, which might be interpreted as a sign of interaction of a fast ($v \sim 10\,000\,\mathrm{km\,s^{-1}}$) shell with circumstellar material. However, the late time interaction scenario is not fully consistent and other interpretations have been proposed, though not proved (cf. Taubenberger et al. 2010). At the same position, only unresolved Hα, [N II] and [S II] lines from an underlying H II region are discernible in SN 1999dn, a sign that there is not (yet) circumstellar material (CSM) interaction. [O I] $\lambda\lambda$6300, 6364 and [Ca II] $\lambda\lambda$7191, 7323 ([O II] $\lambda\lambda$7300, 7330) are clearly visible, with a [Ca II]/[O I] flux ratio of 0.55 ± 0.10.

5 DISCUSSION

SN 1999dn was extensively studied in the last decade, but our new data allow a better determination of the main parameters (cf. Table 4). The light curve results to be 0.5 mag brighter ($M_V = -17.2$) than previously estimated, but still fainter than the average of SNIb/c ($M_V = -17.70$, $H_0 = 72\,\mathrm{km\,s^{-1}\,Mpc^{-1}}$; Richardson et al. 2006). The multicolour observations (Section 3) have shown a relatively strong NIR flux. This large NIR flux is intrinsic, since the EW(NaID), the broad-band colours and the SED all suggest SN 1999dn to be only mildly reddened [$E(B-V) = 0.1$, cf. Section 3.1]. The NIR accounts for about 50 per cent of the flux during the

advance photospheric phase. The bolometric light curve reaches the same luminosity as SNe 2007gr and 1999ex, but is brighter than SN 2007Y, and has a width similar to that of SN 2004aw (cf. Fig. 5). It is known that the peak luminosity gives hints on the ejected ^{56}Ni mass, while the width carries information on the total mass of the ejecta and kinetic energy. To extract in a self-consistent manner information on the ejected mass (M_{ej}), the nickel mass, [M(^{56}Ni)] and the kinetic energy (E_K), we have employed a toy model of the bolometric light curve (Valenti et al. 2008b). Our procedure is based on a two-component analytical model to account for the photospheric and nebular phases. During the photospheric phase ($t \leq 30\,\mathrm{d}$ past explosion), a homologous expansion of the ejecta, spherical symmetry and a concentration of the radioactive ^{56}Ni exclusively in the core are assumed (Arnett 1982). At late times ($t \geq 60\,\mathrm{d}$ past explosion), the model includes the energy contribution from the ^{56}Ni–^{56}Co–^{56}Fe decay, following the works of Sutherland & Wheeler (1984) and Cappellaro et al. (1997). The incomplete trapping of γ-rays and positrons have been accounted for using the Clocchiatti & Wheeler (1997) prescriptions for both photospheric and nebular phases. The bolometric light-curve model suggests a ^{56}Ni mass M(^{56}Ni) = 0.11 M$_\odot$. A comparison with the values from table 2 of Hunter et al. (2009), obtained with similar methods, shows indeed that M(^{56}Ni) is marginally larger than in SN 2007gr (0.076 M$_\odot$), and SN 2007Y (0.06 M$_\odot$, Stritzinger et al. 2009), but smaller than 2004aw (0.3 M$_\odot$). Using an average opacity of 0.06 g cm^{-1} (as in Valenti et al. 2008b) and a scale velocity $v_{\mathrm{sc}} = v_{\mathrm{ph}} = 10\,100\,\mathrm{km\,s^{-1}}$, we obtain an ejected mass $M_{\mathrm{ej}} = 4$–6 M$_\odot$ and kinetic energy $E_K = 5.0$–7.5×10^{51} erg. Surprisingly, but not totally unexpected because of the broadness of bolometric light curve of SN 1999dn, these values are comparable to those obtained for the energetic SN 2008D associated to an X-ray flash (Mazzali et al. 2008). In fact, our toy model makes use of the scale velocity of the explosion ($v_{\mathrm{sc}} = v_{\mathrm{ph}}$, which are similar for SNe 1999dn and 2008D) without taking into account possible differences in the density profiles.

In the case of SN 1999dn, this may cause an overestimate of the physical parameters, the real values being at the lower boundary of those ranges. A more precise determination should rely on more detailed codes. A comparison between the physical parameters deduced, for a sample of well studied SNIb, with our toy model with those derived by more sophisticated codes will be given in Valenti et al. (in preparation). Anyway, even considering the possibility that some physical values for SN 1999dn are slightly overestimate, the SN seems to belong to the group of relatively massive and energetic SNe Ib.

We noted in Section 4.1 that the evolution of the photospheric velocity of SN 1999dn (as well as those of He I and H) are in general very similar to those of other SNIb which implies, following Branch et al. (2002), comparable density profiles, masses and kinetic energies above the photospheres. As noted by those authors, the strong similarity does not leave much room for asymmetries in SNIb, which is confirmed by the [O I] line profile of SN 1999dn at late time (Taubenberger et al. 2009). Only the earliest (–6 d) measurement of the Fe II velocity is significantly larger than the power-law fit by Branch et al.

The previously available spectra of SN 1999dn before and after maximum light have been extensively modelled by means of both the highly parametrized SYNOW (Deng et al. 2000; Branch et al. 2002) and the more sophisticated non-LTE PHOENIX codes (Ketchum et al. 2008; James & Baron 2010). The latter successfully reproduces all main features of the spectra with a homogeneous stellar atmosphere of H, He, C, N, Ne, Na, Mg, Si, Ca and Fe with the

main features identified as He I, O I, Ca II and Fe II at all epochs. Also the He I absorptions were successfully reproduced including γ-ray deposited by the radioactive β decay of ^{56}Co.

Our new spectra confirm the presence of evolving features around 6200 Å during the first weeks (Section 4). Up to maximum light, the region is dominated by a broad and strong feature which, if attributed to H, implies expansion velocities of about 17 000 km s^{-1} (cf. Section 4.1 and Fig. 7). At subsequent epochs (from days +6.8 to +21) our new, superior quality spectra confirm the presence of minor features (cf. Ketchum et al. 2008) in the same region. Whether these components are due to H is not clear but the detection in the highest S/N spectra of weak absorptions at the same velocities with respect to Hβ seems to support the existence of two H layers, one detached at velocities $v = 17\,000$–$13\,000$ km s^{-1}, comparable to that of H in other SNIb (Branch et al. 2002), the other only marginally faster than He I [$\Delta(v) \sim 1500$ km s^{-1}; cf. Fig. 9] and possibly located in the outer He layer. The high Fe II velocity at the earliest epoch (–6 d) seems compatible with the existence of high-velocity H-rich layers.

SN 2007Y and other SNIIb show evidence of interaction of the fast expanding H-rich layer with the CSM (Fig. 11, bottom) about 1 yr past maximum light. This is not the case in SN 1999dn, indicating that no major mass-loss episodes have occurred in the last decade before the explosion [assuming wind velocities $\sim$2000 km s^{-1}, typical of WR progenitors]. There is also no evidence of dust formation at any time, neither from photometric (light and colour curves) nor from spectroscopic observations (line positions and shapes).

On the spectrum obtained at WHT on 1999 September 9, we have measured the O3N2 index (Pettini & Pagel 2004) of the region adjacent to SN 1999dn along the slit of the spectrograph, corresponding to projected linear distance of $\sim$200 pc at the adopted distance of the SN. Relation (3) of Pettini & Pagel (2004) thus provides an oxygen abundance at the SN location $12 + \log(O/H) = 8.39 \pm 0.05 \pm 0.25$ (where the first error is statistical and the second one is the 95% spread of the calibrating relation), which is in excellent agreement with the estimate of Modjaz et al. (2010) (8.32) and slightly lower than the solar abundance $12 + \log(O/H) = 8.69 \pm 0.05$ (Asplund et al. 2009) and close to the average metallicity derived for the sites of a sample of fifteen SNIb, which also includes SN 1999dn, studied in Modjaz et al. (2010).

A search for the progenitor of SN 1999dn has been carried out on *Hubble Space Telescope* archive images (Van Dyk et al. 2003). The progenitor was not detected down to $M_V^o \geq -7.3$ mag and $(U - V)^o \leq 2.5$ mag [these values do not change significantly with our assumptions on H$_0$ and $E(B - V)$] . Unfortunately, this determination does not strongly constraints the nature of the progenitor either as a massive, single WR star (e.g. $M_{ZAMS} \geq 23$–25 M$_\odot$ at $Z = 0.02$; Georgy et al. 2009), or as a star of lower initial mass in an interacting binary system (e.g. $M_{ZAMS} \geq 14$–16 M$_\odot$ at $Z = 0.02$; Yoon, Woosley & Langer 2010). However the lack of signatures of dust favours the single, massive star scenario, given the fact that while the radiation field of single WR stars is expected to prevent dust formation in their local environment, while binarity in WR stars seems to provide the necessary physical conditions for it (Crowther 2007, and references therein).

The moderate metallicity environment ($12 + \log(O/H) \sim 8.4$, slightly sub-solar) in which SN 1999dn exploded is not inconsistent with the single scenario. In fact, the binary channel for producing WR stars in WR galaxies (as NGC7714) is important just at lower $[12 + \log(O/H) < 8.2]$ metallicity (e.g. Lopez-Sanchez & Esteban 2010), while the probability of forming single WR stars increases with the metallicity because it is easier to reach the WR phase due to

the metallicity-dependence of the stellar wind (e.g. Lopez-Sanchez & Esteban 2010, and references therein). The lower mass limit for having a WR progenitor decreases from $\sim$40–50 M$_\odot$ at $Z = 0.004$ to $\sim$23.–25 M$_\odot$ at $Z = 0.02$ (Georgy et al. 2009). As a consequence, the progenitor of SN 1999dn could be a single WR star having a main-sequence mass $\geq$23–25 M$_\odot$.

Also the relatively small flux ratio [Ca II]/[O I] = 0.55 ± 0.10, known for being constant with time (cf. the spectra collection by Taubenberger et al. 2009) is consistent with a single massive star scenario. In fact, Fransson & Chevalier (1987, 1989) have shown that this ratio is a diagnostic of the core mass of the progenitor, with higher ratios indicative of smaller cores. The ratios measured for SN 1993J, SN 2007Y and SN 2008ax are 0.6, 1.0 and 0.9, respectively (Stritzinger et al. 2009; Taubenberger et al. 2010). Since the core mass is strongly dependent on the progenitor zero-age main sequence (ZAMS) mass, thus we have an indication that the progenitor of SN 1999dn is more massive than the above mentioned SNe.

6 CONCLUSIONS

We have presented detailed photometric observations and new spectra of SN 1999dn from before maximum to the nebular phase. These new data turn this object, already considered a prototypical SNIb, into one of the best observed objects of this class.

SN 1999dn was a moderately faint SNIb ($M_V = -17.2$ mag) which produced 0.11 M$_\odot$ of ^{56}Ni. With a toy model, we have estimated an ejected mass of 4–6 M$_\odot$ with $E_K = 5.0$–7.5×10^{51} erg. Due to the rough approximation of the model, these values may be slightly overestimated. Our analysis on SN 1999dn confirms that, contrary to early belief, a prototypical SN Ib may produce several foe of kinetic energy and eject several solar masses.

Overall, the main parameters of the explosion are comparable to those of the Type Ic SN 2004aw and the massive Type Ib SN 2008D, much higher than those of the low-energy and low-ejected-mass SN 2007Y. Higher explosion energy and ejected mass, along with the small flux ratio [Ca II]/[O I], the lack of signatures of dust formation and the relatively high-metallicity environment point towards a single massive progenitor ($M_{ZAMS} \geq 23$–25 M$_\odot$). On the other hand, none of these evidences completely rules out the scenario of a less massive star in a binary system.

The spectra of SN 1999dn at various epochs are similar to those of other SE SNe that show clear presence of H at early (Type IIb SNe 1993J and 2008ax, Type Ib SNe 2000H, 2007Y and 1999ex) or late (SNe 1993J, 2008ax, 2007Y) epochs. Such similarities, coupled to the fact that accurate spectral modelling (e.g. Ketchum et al. 2008) did not find other satisfactory explanations for the puzzling 6200-Å feature, lead us to support its identification with detached Hα. We conclude, therefore, that it is likely that residual H can be recognized in the spectra of most SNIb if observed sufficiently early on.

REFERENCES

Anderson J. P., James P. A., 2008, MNRAS, 390, 1527
Arnett W. D., 1982, ApJ, 253, 785
Asplund M., Grevesse N., Sauval A. J., Scott P., 2009, ARA&A, 47, 481
Ayani K., Furusho R., Kawakita H., Fujii M., Yamaoka H., 1999, IAU Circ., 7244, 1
Barbon R., Benetti S., Cappellaro E., Patat F., Turatto M., Iijima T., 1995, A&AS, 110, 513
Branch D. et al., 2002, ApJ, 566, 1005
Cappellaro E., Mazzali P. A., Benetti S., Danziger I. J., Turatto M., della Valle M., Patat F., 1997, A&A, 328, 203
Chevalier R. A., Soderberg A. M., 2010, ApJ, 711, L40
Chornock R. et al., 2010, ApJ, preprint (arXiv:1001.2775)
Clocchiatti A., Wheeler J. C., 1997, ApJ, 491, 375
Clocchiatti A., Wheeler J. C., Brotherton M. S., Cochran A. L., Wills D., Barker E. S., Turatto M., 1996, ApJ, 462, 462
Crowther P. A., 2007, ARA&A, 45, 177
Deng J. S., Qiu Y. L., Hu J. Y., Hatano K., Branch D., 2000, ApJ, 540, 452
Desroches L. B., Wang X., Ganeshalingam M., Filippenko A., 2007, Cent. Bureau Electron. Telegram 1001
Dessart L. et al., 2008, ApJ, 675, 644
Elmhamdi A., Danziger I. J., Cappellaro E., Della Valle M., Gouiffes C., Phillips M. M., Turatto M., 2004, A&A, 426, 963
Filippenko A. V., 1982, PASP, 94, 71
Filippenko A. V. et al., 1995, ApJ, 450, L11
Fransson C., Chevalier R., 1987, ApJ, 322, 15
Fransson C., Chevalier R., 1989, ApJ, 343, 323
Freedman W. L. et al., 2001, ApJ, 553, 47
Folatelli G. et al., 2006, ApJ, 641, 1039
Fynbo J. P. U. et al., 2004, ApJ, 609, 962
Galama T. J. et al., 1998, Nat, 395, 670
Georgy C., Meynet G., Walder R., Folini D., Maeder A., 2009, A&A, 502, 611
Hakobyan A. A., Petrosian A. R., McLean B., Kunth D., Allen R. J., Turatto M., Barbon R., 2008, A&A, 488, 523
Hamuy M. et al., 2002, AJ, 124, 417
Harutyunyan A. H. et al., 2008, A&A, 488, 383
Heger A., Fryer C. L., Woosley S. E., Langer N., Hartmann D. H., 2003, ApJ, 591, 288
Hjorth J. et al., 2003, Nat, 423, 847
Hunter D. et al., 2009, A&A, 508, 371
James S., Baron E., 2010, ApJ, 718, 957
Kandrika H., Li W., 2007, Cent. Bureau Electron. Telegram 997
Ketchum W., Baron E., Branch D., 2008, ApJ, 674, 371
Kraan-Korteweg R. C., 1995, VizieR On-line Data Catalog, 7098, 0
Landolt A. U., 1992, AJ, 104, 340
Li W. et al., 2010, MNRAS, submitted (arXiv:1006.4612)
Lopez-Sanchez A. R., Esteban C., 2010, A&A, 516A, 104L
Malesani D. et al., 2004, ApJ, 609, L5
Matheson T., Filippenko A. V., Li W., Leonard D. C., 2001, ApJ 121, 1648
Mattila S., Meikle P., Walton N., Greimel R., Ryder S., Alard C., Lancon A., 2002, IAU Circ., 7865, 2

Mazzali P. A. et al., 2008, Sci, 321, 1185
Modjaz M. et al., 2006, ApJ, 645, L2
Modjaz M. et al., 2009, ApJ, 702, 226
Modjaz M., Bloom J. S., Filippenko A. V., Kewley L., Perley D., Silverman J. M., 2010, ApJL, submitted (arXiv:1007.0661v1)
Pastorello A., Turatto M., Rizzi L., Cappellaro E., Benetti S., Patat F., 1999, IAU Circ., 7245
Pastorello A. et al., 2008, MNRAS, 389, 955
Pettini M., Pagel B. E. J., 2004, MNRAS, 348, L59
Pian E. et al., 2006, Nat, 442, 1011
Qiu Y. L., Qiao Q. Y., Hu J. Y., 1999a, IAU Circ., 7241
Qiu Y. L., Huang l., Yao B., Li H., 1999b, IAU Circ., 7244
Roming P. W. A. et al., 2009, ApJ, 704, L118
Richardson D., Branch D., Baron E., 2006, AJ, 131, 2233
Richmond M. W. et al., 1996a, AJ, 111, 327
Richmond M. W., Treffers R. R., Filippenko A. V., Paik Y., 1996b, AJ, 112, 732
Schlegel D. J., Finkbeiner D. P., Davis M., 1998, ApJ, 500, 525
Skrutskie M. F. et al., 2006, AJ, 131, 1163
Soderberg A. M. et al., 2008, Nat, 453, 469
Stritzinger M. et al., 2002, AJ, 124, 2100
Stritzinger M. et al., 2009, ApJ, 696, 713
Sutherland P. G., Wheeler J. C., 1984, ApJ, 280, 282
Taubenberger S. et al., 2006, MNRAS, 371, 1459
Taubenberger S. et al., 2009, MNRAS, 397, 677
Taubenberger S. et al., 2010, MNRAS, submitted
Turatto M., Rizzi L., Salvo M., Cappellaro E., Benetti S., Patat F., 1999, IAU Circ., 7244
Turatto M., Benetti S., Cappellaro E., 2003, in Hillebrandt W., Leibundgut B., eds, From Twilight to Highlight: The Physics of Supernovae. Proc. ESO/MPA/MPE Workshop. Springer-Verlag, Berlin, p. 200
Turatto M., Benetti S., Pastorello A., 2007, Immler S., Weiler K., McCray R., eds AIP Conf. Proc. Vol. 937, Supernova 1987A: 20 years after: Supernovae and Gamma-Ray Bursters Am. Inst. Phys., New York, p. 187
Valenti S. et al., 2008a, ApJ, 673, L155
Valenti S. et al., 2008b, MNRAS, 383, 1485
Van Dyk S. D., Peng C. Y., Barth A. J., Filippenko A. V., 1999, AJ, 118, 2331
Van Dyk S. D., Li W., Filippenko A. V., 2003, PASP, 115, 1
Weedman D. W., Feldman F. R., Balzano V. A., Ramsey L. W., Sramek R. A., Wu C.-C., 1981, ApJ, 248, 105
Wheeler J. C., Levreault R., 1985, ApJ, 294, L17
Woosley S. E., Eastman R. G., 1997, in Ruiz-Lapuente P., Canal R., Isern J., eds, Thermonuclear Supernovae, NATO ASI Series Vol. 486, Kluwer, Dordrecht, p. 821
Yoon S.-C., Woosley S. E., Langer N., 2010, preprint (arXiv:1004.0843)

This paper has been typeset from a TEX/LATEX file prepared by the author.